Microwave Resonant Cavities

In the Search for Dark Matter Axions

Carisa Miller

Department of Physics, University at Albany
University of Washington INT REU

Advisor: Leslie Rosenburg

Abstract

As a solution to both the strong CP problem and the unknown composition of dark matter, axions present themselves highly motivated theoretical particles. The most promising methods of detecting axions is the use of a tunable microwave resonant cavity such as that in place in ADMX. In order to extend the current search range of ADMX, and to study cavity mode structures, three cavities of similar geometries were constructed and tested. Simple tests confirmed the expanded search range as well as well expected frequencies. Further tests provided comprehensive illustrations of the mode behavior in each cavity.

1 Introduction

The existence of the axion would have profound effects on both cosmology and particle physics, resolving at once two of the problems within these fields. In order to introduce the motivation behind the theory of the axion, Section 1.1 will give a brief consideration of CP violation and the strong CP problem as well as the presence and unknown composition of dark matter in the Universe. Section 1.2 will then discuss the axion as a possible solution to both of these problems.

1.1 A Brief Discussion of the Strong CP Problem and Dark Matter

1.1.1 CP Violation and the Strong CP Problem

In quantum chromodynamics (QCD) – the gauge theory of string interactions – the Lagrangian is usually written as [1]:

$$\mathcal{L}_{QCD} = -\frac{1}{4}\left(G^{a}_{\mu\nu}\right)^{2} + \bar{\psi}_i(i\gamma^{\mu}D_{\mu} - m)\psi_i \quad (1.1)$$

where the ψ are Dirac fields each depicting a massive quark and the tensors $G^a_{\mu\nu}$ are the field-strength tensors of a gluon. Both terms in this Lagrangian are invariant under charge conjugation parity (CP) symmetry. There is also an additional term, often ignored, called the "theta vacuum term":

$$\mathcal{L}_\theta = \theta \frac{{g_s}^2}{32\pi^2} G^a_{\mu\nu} \bar{G}_{a\mu\nu} \qquad (1.2)$$

where g_s is a coupling constant and θ is a free parameter between 0 and 2π. This term violates both time (T) and parity (P) symmetries, but not charge conjugation (C) symmetry, thus, it violates CP.

One way this CP violation has been searched for in QCD is by investigating the neutron electric dipole moment. Current experimental bounds on the neutron EDM ($d_n < \sim 10^{-25}$ e cm) imply an unnaturally small value for θ ($\sim 10^{-9}$) [2]. The fine tuning problem of how to make θ exceptionally small is, in essence, the Strong CP Problem.

1.1.2 Dark Matter

Much evidence has been found that suggests the presence of a substance of unknown composition in the Universe. Only inter-acting gravitationally with "normal" matter, this substance neither emits nor absorbs electro-magnetic radiation, and thus is termed "dark matter".

Strongest indications of dark matter come from the examinations of galactic rotation curves. An example of such a curve is shown in Figure 1 [3]. The graph plots the distance of matter from a galaxy's center against its tangential velocity. The line labeled "disk" is the curve expected from observed luminous matter, while the plotted dots are what was actually measured. From this large inconsistency between the two, there can be inferred a "halo" of dark matter within the galaxy.

While "normal" baryonic matter has been ruled out as a component of dark matter, several different candidates have been suggested to explain the composition of dark matter, including supersymmetric particles, massive neutrinos, axions, and others. Among these prospective ideas, two broad categories can formed: hot dark matter and cold dark matter. The main distinction between the two is that "hot" dark matter (HDM) components would have been travelling at high velocities in the early Universe, while "cold" dark matter (CDM) particles would have travelled sub-relativistically. The latter would have allowed for small scale structures in the Universe to form first, in what is referred to as a "bottom – up" manner, as opposed to HDM which would have caused the Universe to form in a "top – down" manner in which large structures would form first [4]. Observations of the current structures in the Universe better support the theory of CDM as the main comprisal of dark matter.

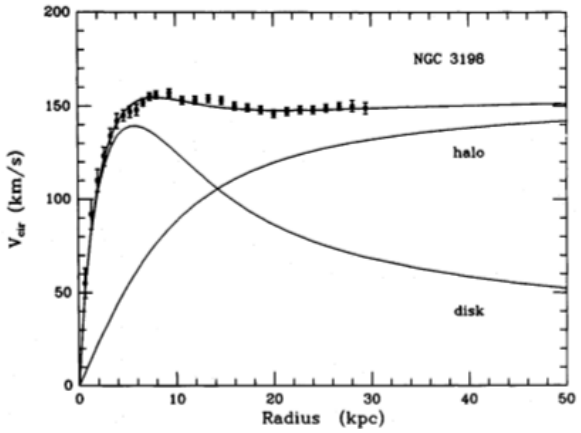

Figure 1: Rotation curve of NGC 3189 showing expected ("disk"), observed ('NGC 3198"), and inferred ("halo") matter in the galaxy.

1.2 Axions

1.2.1 Axions as a Solution to the Strong CP Problem

As a solution to the strong CP problem, Peccei and Quinn [5] posited a new global symmetry, with the effect of turning the parameter θ into a field. This new PQ symmetry, when spontaneously broken, forces θ to zero, cancelling the CP violating term of the QCD Lagrangian, providing consistency with experimental observation.

It was later shown by Weinberg [6] and Wilczek [7] that this new symmetry would be manifested as a new particle. This new particle, the axion, has a (undetermined) non-zero mass, making it a psuedo-Goldstone boson.

1.2.2 Axion as Cold Dark Matter Candidates

Theories for the production of dark matter axions include thermal production, misalignment production, and the decay of axion strings.

Several experiments have narrowed the window of the axion mass range and within this window thermal production of axions would unable to account for any sizable portion of dark matter. As well, thermal production of axions forms HDM axions which is inconsistent with the preferred theory of CDM.

The theory of misalignment production forms CDM, as favored. A brief explanation of this mechanism is as follows: Under the conditions of the early universe, the PQ symmetry was unbroken, allowing all values of θ to be probable. As the universe expanded and cooled, it reached a point at which conditions cause breaking of the PQ symmetry, and the field descends down to and oscillates about the point $\theta = 0$, corresponding to a zero-momentum condensate of axions. These axions, out of thermal equilibrium with the baryonic matter due to their very weak interactions, remain cold. Eventually the axions, originally uniformly distributed, fall into the gravitational potential wells of clustered baryonic matter and could comprise a substantial fraction of the dark matter observed today.

The theory of the decay of axion strings does not, as of yet, provide a dependable estimate of the mass and density of dark matter axions produced through this mechanism. As such, it is unclear of the contribution of string decay to the present axion density [1, 8].

2 Background

This section will discuss the use of microwave resonant cavities in the detection of axions, and also how this method is applied to ADMX.

2.1 Using Resonant Cavities to Search for Dark Matter Axions

The current mass search window for axions is between 10^{-3} eV and 10^{-6} eV [8]. Within this range, the coupling of axions to photons is expected to be very weak. Also within these constraints, axions are expected to have a number density of approximately 10^{15} per cc with a mean lifetime of $\sim 10^{42}$ years.

Their exceptionally long lifetime and weak coupling make axions very difficult to detect, so much so that they were dubbed “invisible” axions. But an experiment purposed by Pierre Sikivie [9] uses the axions ability to convert into two photons (one real, and one virtual) through the Primakoff effect by using a

resonant cavity of high quality factor placed in a strong, externally-applied magnetic field, to excite the axion to resonant conversion when the cavity resonates at a frequency corresponding to the axion mass.

The main mode for axion detection is the TM_{010} which has a longitudinal electric field parallel to the applied magnetic field. The resonant frequency of this mode (and all others) depends on the geometry of the cavity. Because the mass of the axion is unknown, the resonant frequency of the cavity must be tunable.

Though axions only interact with TM modes, the tuning capability of the cavity is still affected by TE and TEM, which have no electric fields in the longitudinal direction. When the bandwidth frequencies of two modes overlap, this is called a mode crossing. Mode crossing are not of consequence until the resonant frequencies of TE and TEM modes are close enough to the TM_{010} mode, at which point data cannot be taken at that frequency.

2.2 ADMX

The resonant cavity used in ADMX is a right circular cylinder with a diameter of approximately 0.5 meters and a height of approximately 1 meter. The cavity is tuned by the insertion of two conducting (or dielectric) rods that are rotated from the edge of the cavity toward the center, raising (lowering) the resonant frequencies.

The power signal of the cavity is received by extremely low-noise amplifiers known as SQUID (Superconducting QUantum Interference Device) amplifiers and delivered to the receiver. The conversion of an axion into a photon would result in a small peak in the observed power spectrum near the resonant frequency.

The necessary strong magnetic field is supplied by an 8 Tesla magnet. The experiment is conducted at cryogenic temperatures to reduce thermal noise while SQUID amplifier reduce electronic noise, both of these factors giving rise to a desired high quality factor, Q – to be discussed briefly in Section 4.2.

3 Design and Construction of Tunable RF Cavities

Objectives, conception, and engineering for the construction a tunable RF cavity to extend the present search range of ADMX into higher frequencies, as well as method used in testing the end product(s) is discussed in the following section.

3.1 Parameters for Design

3.1.1 Objectives

The cavity of this experiment was to be tuned by a single rod moving from the wall, circularly, into the center and back outward again. Constraints for design began with an intended tuning range of the TM_{010} mode somewhere within 2 – 5 GHz, which provided the precursory dimensions of the cavity diameter. Following that, the necessity of minimizing mode crossings in the vicinity of the TM_{010} mode needed to be addressed. For this, various cavity lengths were examined as the TM_{010} mode is unaffected by length and would remain at the desired frequency while the TE and TEM modes are affected by length and can be tuned accordingly to minimize mode crossings. Also considered in design was that the importance that the cavity be of a material of high electrical

conductivity and the preference that it be able to be easily installed with the current ADMX setup.

3.1.2 Design

With the help of an RF cavity solving program "Poisson Superfish" [10] many cylindrical cavity geometries were modeled in order to find a cavity design of suitable tuning range. The absolute upper limit of the range could not exceed 4.5 GHz due to the limitations of the frequency measurement capabilities of the network analyzer – a device that provided a variable frequency source and measured the ratio of the power between the transmitted and received signal. Modeling bare cavities of different diameters gave the lower limit of the tuning range, while modeling the cavities with rods at the center gave the upper limit of the tuning range, which also depended on the size of the rod. From the calculated frequencies provided by the program, in cavities with appropriate diameters corresponding to the desired lower limit, the upper limits of the tuning range within the same cavity were reachable only with rod sizes of disproportionately large diameters that would not feasibly allow for the cavity to be estimated as empty when the rod was positioned at the edge, and as such also rendered the calculation of the lower limit of the frequencies provided under this assumption incorrect.

When considering the optimal cavity and rod diameters, consideration had to be taken to weigh the maximizing of the tuning range against reasonable rod sizes. It was determined that a cavity with a diameter of 8 cm (~3.15 in) and a tuning rod of 1cm (~0.4 in) was the best cavity to fit these factors. It was also decided that three separate cavities of different lengths – 5, 10, and 20 inches[1] – would be constructed in order to have varying TE and TEM mode structures and be able to take data at all frequencies of the TM_{010} mode.

Copper was decided to be the primary material for constructing the cavities as well as the rods for each and the end caps that were to be designed to be interchangeable between the cavities. OFHC (Oxygen Free High Conductivity) copper, specifically, was chosen for its purity and, as such, its superior electrical and thermal conductivity.

An adapter plate was designed to mimic the top plate of the current ADMX cavity, thus fitting with the current supports. The plate was designed to appropriately position the cavities beneath the gear boxes already in place for one of the ADMX tuning rods, and also made use of the ADMX antenna probes. Additional simple considerations were made for a heat sink and multiple temperature sensors and the support of a counterweight to avoid torque on the ADMX hardware as cavities would be placed off center. The adapter plate was also to be made of OFHC copper.

3.2 Construction

3.2.1 Material Accessibility

When looking into the purchase of OFHC copper in order to construct the cavities it was found that pipes of 3½ in. inner diameter were readily available. While not exactly of the diameter intended, the time and effort saved by

[1] In the following sections the cavities corresponding to these lengths will be referred to often as "small," "medium," and "large," respectively.

not needing to machine the cavities made this dimensional sacrifice well worth it. A small forfeit was made in the rod size as well when $^{5}/_{16}$ in. diameter rods were also chosen for their convenient availability as well.

3.2.2 Modeling

Before beginning construction, the final designs were modeled in Autodesk® Inventor® [11]. The design of the adapter plate was used as a template to be given a professional to construct as the dimensions needed to be exact in order for the plate to fit within the ADX hardware. The following images are samples of the inventor models.

Figure 2 shows the medium cavity assembled with the top and bottom end caps. The end facing outward has holes for the tuning rod and antenna probe. Unseen on the bottom end cap is a hole for a second antenna. The ring of holes around the edge fit sixteen threaded rods that are to serve the dual purpose of supporting the cavity when it is finally installed into ADMX, and providing a tight seal when each cavity is eventually fitted with its own permanent end caps.

Figure 3 shows the large cavity and end caps as they would look assembled and supported beneath the adapter plate.

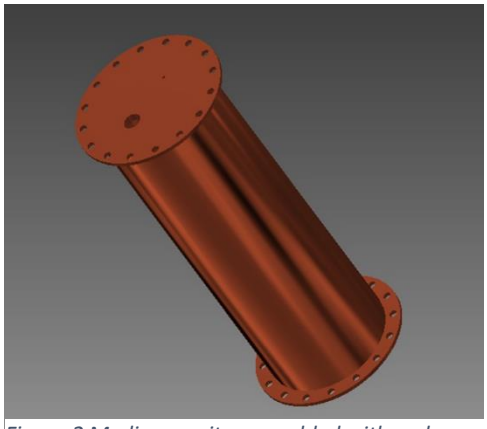

Figure 2 Medium cavity assembled with end caps, as modelled in Inventor®.

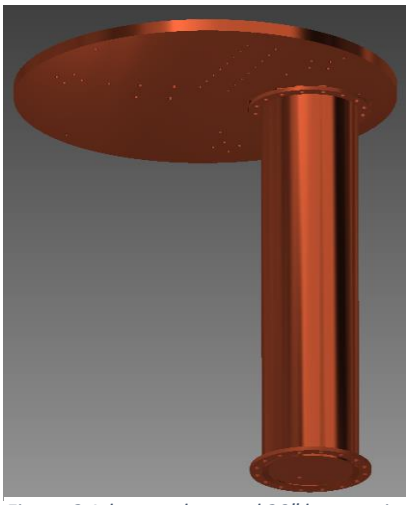

Figure 3 Adapter plate and 20" long cavity as modeled in Inventor®.

3.2.3 Construction

The adapter plate was constructed by the CENPA Machine Shop. The cavities, end plates, and tuning rods, were constructed by Jim

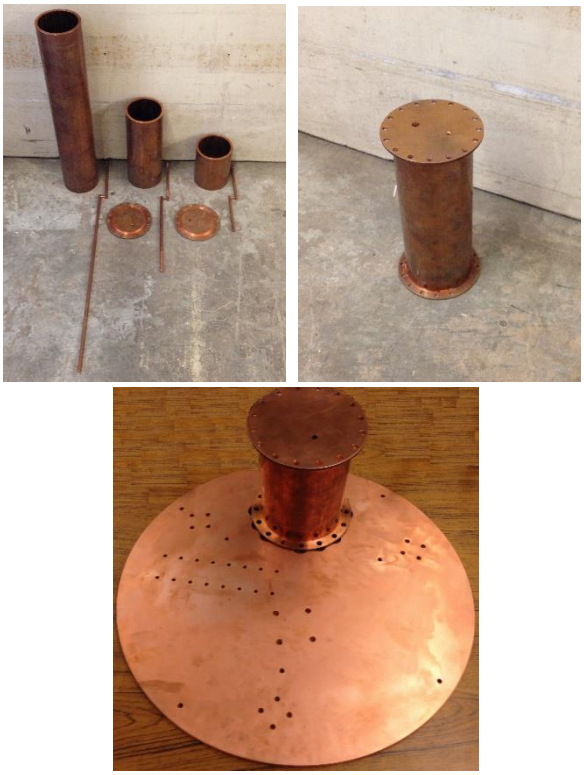

Figure 4 (Top left) all three cavities, end caps, and tuning rods, (top right) medium cavity, and (bottom) small cavity and adapter plate.

Sloan and myself in the CENPA student shop. The end result are shown in the figures below.

Figure 4 shows all three cavities, their tuning rods, and the inter-changeable end caps, the medium cavity assembled with the end caps, much as it appears in the previous *Inventor* model, and the adapter plate and the small cavity positioned as it would be for testing in ADMX.

3.3 Testing

When testing the cavities, the setup was very similar to the sketch shown in Figure 5, with the exception that the port was located at the bottom of the cavity. With an antenna in the bottom port, another antenna was extended into the cavity only so far as to weakly couple the two. As the frequency of the source varied, the network analyzer gave the transmitted power (in decibels) of the swept response.

Preliminary tests were run on the bare cavities and used to identify various TM and TE modes, as discussed below. Later tests were run on the cavity with the rod positioned, stationary, at the wall and again at the center to confirm the expected tuning range. Finally, the rods were attached to a stepper motor and data was taken as the rods rotated and the cavity was tuned. Figure 6 show the large cavity, with stepper motor, and the network analyzer during the final tests.

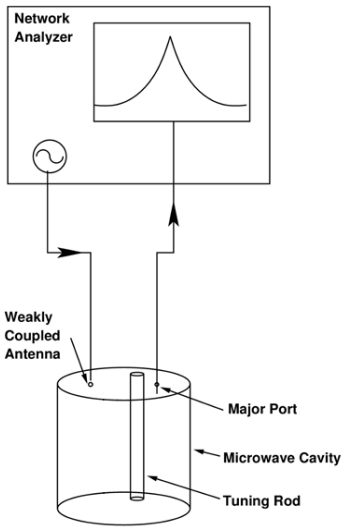

Figure 5 Sketch of the cavity testing setup.

Figure 6 Testing setup of the large cavity as it is being tuned.

4 Results and Discussion

4.1 Preliminary Results

4.1.1 Bare Cavities

Initial tests were done to yield plots of the mode frequencies of the bare cavities which shown on the following page in Figure 7. On each of the graphs, the frequency in the cavity is plotted along the horizontal axis against the

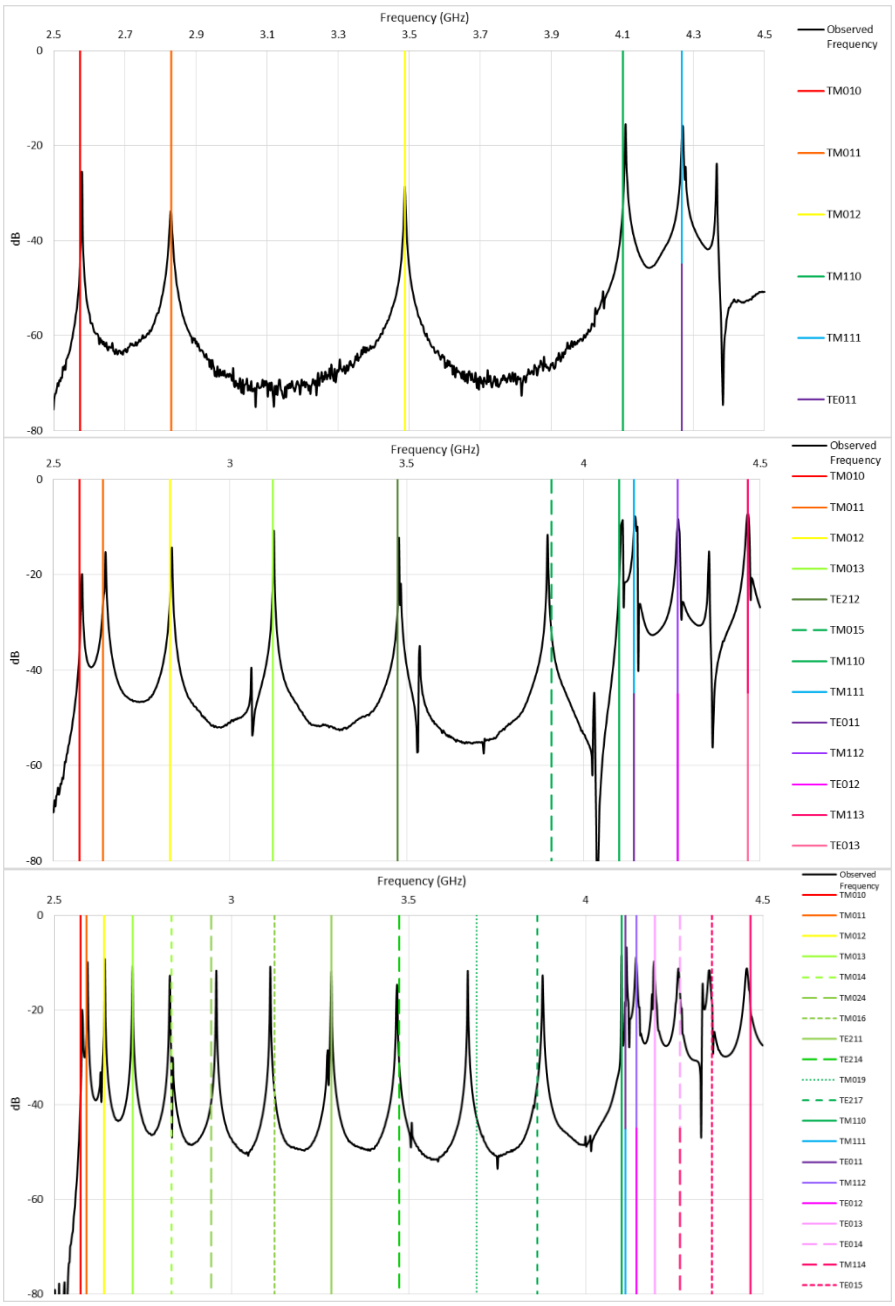

Figure 7 Plots of the transmitted power versus frequency for the empty (top to bottom) small, medium, and large cavities.

transmission (in dB) along the vertical axis. The black lines are the swept response of the cavities and the colored vertical lines mark the expected frequencies of various TE and TM modes. Expected frequencies were obtain by the simple application of Maxwell's equations to an ideal right circular cylinder.

As the above figure shows, the observed peaks are in excellent agreement with their corresponding expected values. Also as expected, the TM_{010} mode was the lowest mode of the cavity and did not change frequency between the different lengths.

4.1.2 Rod Inserted

After confirming that the results agreed with calculations, the tuning rods were inserted and data was taken twice again with each cavity; once with the rod held stationary at the edge, and once with it held stationary at the center. The figure on the following page shows all six graphs generated in this process.

The top row of graphs in Figure 8 show the swept response of the small, medium, and large cavities, respectively, with the rod at the edge, while the bottom row shows the measurements with the rod at the center. The red points on each graph indicate the peaks of the TM_{010} mode.

Comparing each top graph with its corresponding bare cavity plot, one can see that, while the introduction of the rods caused minor changes in the mode structures, the effect was not so much as to render our estimation of the cavity as bare invalid. And comparing each

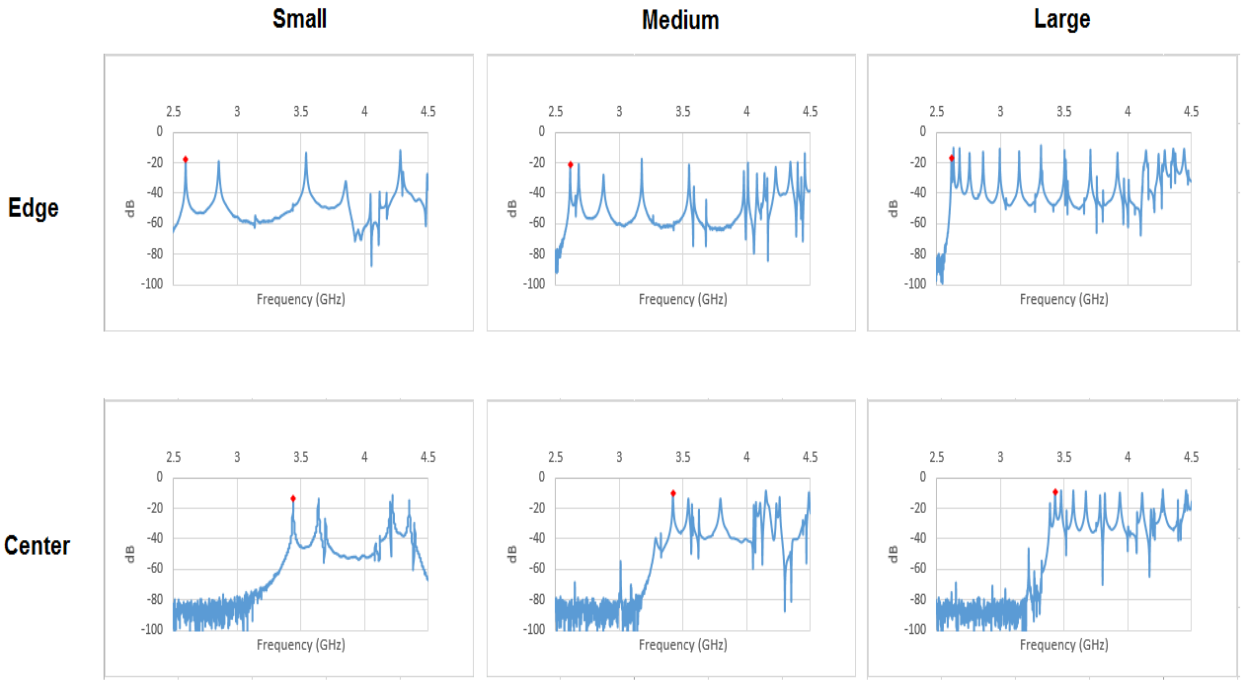

Figure 8 Data taken with the rod at the edge (top) and center (bottom) of the small (left), medium (middle), and large (right) cavities. A red dot marks the TM_{010} mode in each plot.

bottom graph with that directly above it, the full tuning range of each cavity can be seen by observing the movement of the TM_{010} peak. It can also be seen that while the mode structure of other various modes is different in each cavity, the TM_{010} mode tunes the same in all three with a range of a little less than 1 GHz.

4.2 Q Factor

Simply a way to measure the losses of a system, the quality factor can be calculated easily from the data by:

$$Q = \frac{f}{\Delta f}$$

where f is the maximum frequency of a peak and Δf is the width of the peak at half the maximum.

Shown to the right is an enlarged view of the TM_{010} peak of the small bare cavity. Using this peak, and taking into account the dB scale, the calculated Q was approximately 2000. While this value was lower than expected, further data should be collected at a higher resolution in order to get a more accurate measurement.

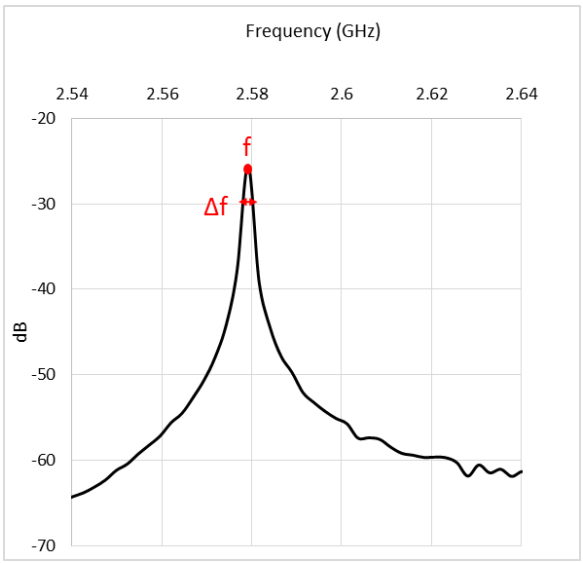

Figure 9 Expanded view of the TM_{010} peak of the small, empty cavity marked at the peak and at half of the maximum. The decibel scale must be accounted for when considering the half maxiumum value.

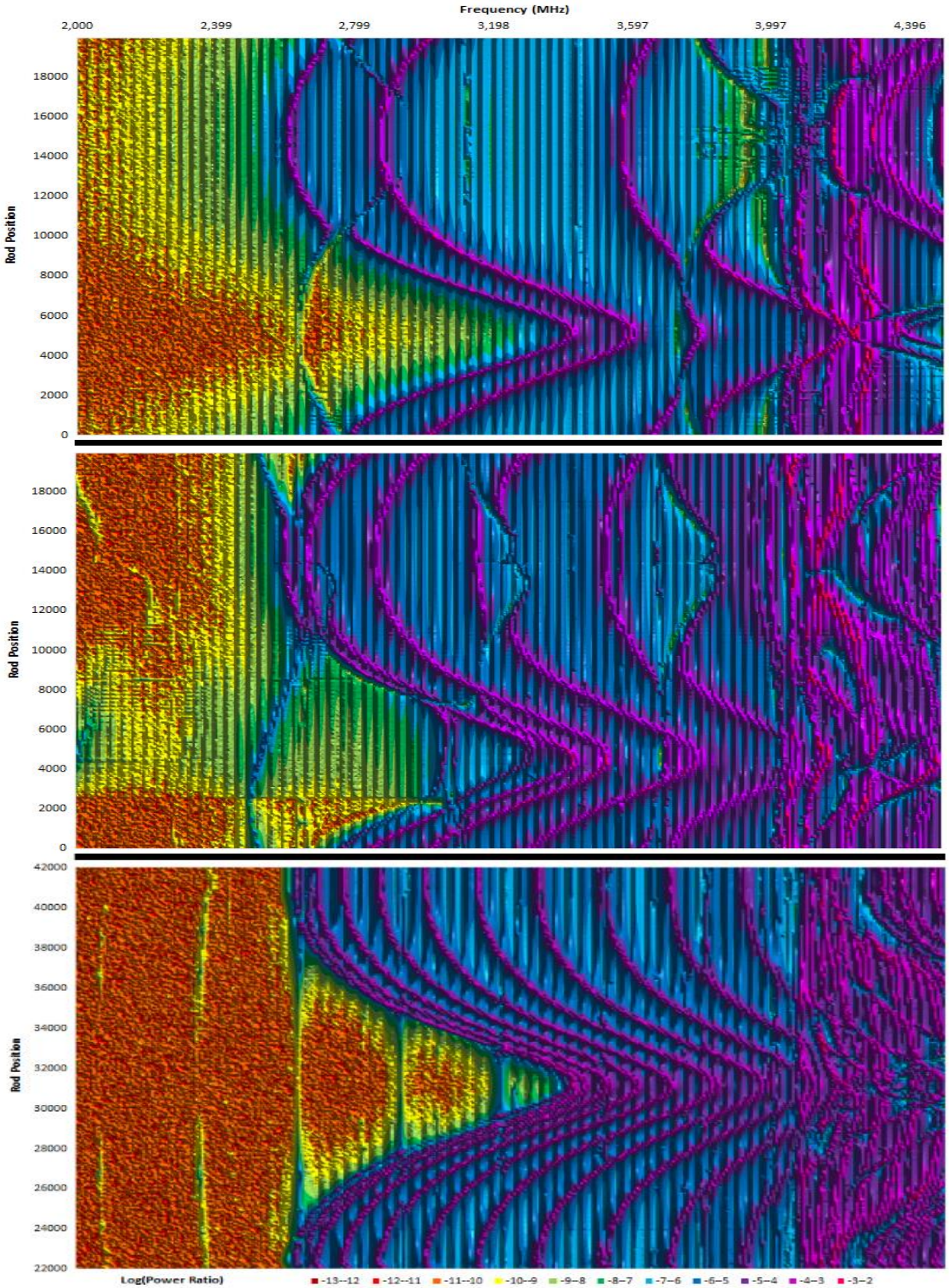

Figure 10 Mode maps of the large (top), medium, and small (bottom) cavities.

4.3 Mode Maps

With all initial tests giving expected results, the final measurement were able to be taken. Data taken as the rod was circulated was used to produced mode maps as a visual of how the modes moved as the cavity was tuned. The mode maps of the small, medium, and large cavities are shown on the previous page in Figure 10. Each map plots the frequency against the rod position (in arbitrary numbers given by the network analyzer), while the color scale represents the power transmission (in dB).

The preceding figure gives valuable, comprehensive information about the movements of the cavities' tunable modes. In each figure, the lowest mode, the TM_{010} mode, can be easily seen moving to higher frequencies as the cavity is tuned. Another thing that these maps show is the highly complicated mode structure in the cavities at high frequencies as the modes become denser.

The complications of other modes can also be a problem even at lower frequencies. In the maps of the small and medium cavities there appears to be modes that are "anti-tuning", while in the large cavity there are modes that don't seem to tune at all. These appear to be TEM modes, as they double in occurrence as the cavity doubles in length as expected of TEM modes. Though TEM modes, are not expected to tune with the cavity, it is believed that the small armature of the rod, as it sweeps around the top of the cavity, appears to change the effective length of the cavity. This would also explain why the effect is so large in the small cavity where, proportionally, the armature is of greater consequence, and almost nonexistent is the large cavity, where the armature contributes much less than the length of the cavity. In the medium cavity the TEM modes have small disturbances at their crests; it is thought that these are the result of another part of the structure, such as the rod or armature, resonating.

The most important information these maps give is where mode crossings with the TM_{010} mode occur. The frequencies at which these crossings occur changes by the length of the cavity, so by constructing multiple cavities, blind spots caused by mode crossings have been effectively eliminated.

5 Conclusion

Three resonant cavities were constructed in order to tune a TM_{010} mode of higher frequency than the current ADMX range. Furthermore, these cavities were of varied lengths so that each cavity's unique mode structure could be used to search frequencies where the other two may have mode crossings. Tests of these cavities confirm their intended search ranges and give comprehensive visual representations of mode behavior.

In order to improve the quality factor, plans have been made to fit each cavity with its own permanent and tightly sealed end caps, to polish or anneal the OFHC copper for higher purity, and to take data at higher resolution. Further considerations have also suggested the implementation of disturbances in the cavity walls in order to disrupt the transverse electric fields of TE and TEM modes and reduce or eliminate mode crossings. Also recommended, for efficiency, is the modification of the adapter plate to be able to support two cavities so both may be tuned simultaneously.

Following the current upgrades underway in ADMX, these cavities may be used within the year to collect data.

6 References

[1] E. J. Daw, Ph.D. thesis, Massachusetts Institute of Technology, 1998.

[2] I.S. Altarev et al., Phys. Lett. B. **276**, 242 (1992)

[3] T. S. van Albada, J. N. Bahcall, K. Begeman, and R. Sanscisi, Ap. J. **295,** 305 (1985).

[4]

[5] R.D. Peccei and Helen R. Quinn, Phys. Rev. Lett. **38**, 1440 (1977)

[6] S. Weinberg, Phys. Rev. Lett. **40**, 223 (1978)

[7] F. Wikczek, Phys. Rev. Lett. **40**, 279 (1978)

[8] D. B. Yu, Ph.D. thesis, Massachusetts Institute of Technology, 2004.

[9] P. Sikivie, Phys. Rev. Lett. **51**, 1415 (1983).

[10] R. F. Holsinger and K. Halbach, (2011). Poisson Superfish (Version 7) [Software]. Available from http://laacg1.lanl.gov/laacg/services/download_sf.phtml

[11] B. Gelfand (2013). Autodesk® Inventor® [Software]. California: Autodesk

7 Acknowledgements

I would like to thank Dr. Leslie Rosenburg for being my mentor this summer. I would like to thank Jim Sloan for being an immense help with my project. I would also like to thank the entire ADMX team for their help as well. I would also like to acknowledge Ron Musgrave and David Hyde who taught me all I know about machining.

For running the REU program I would like to thank Dr. Alejandro Gracia, Dr. Subhadeep Gupta, Linda Vilett, and Janine Nemerever. And for this entire opportunity, I would like to thank the NSF and the University of Washington.